BULLETIN OF THE POLISH ACADEMY OF SCIENCES
TECHNICAL SCIENCES, Vol. 71(2), 2023, Article number: e144614
DOI: 10.24425/bpasts.2023.144614

Influence of annealing conditions on changes of the structure and selected properties of $Al_{88}Y_7Fe_5$ and $Al_{88}Y_6Fe_6$ alloys

Rafał BABILAS[1], Monika SPILKA[1]*, Wojciech ŁOŃSKI[1], Adrian RADOŃ[2], Mariola KĄDZIOŁKA-GAWEŁ[3], and Piotr GĘBARA[4]

[1] Faculty of Mechanical Engineering, Silesian University of Technology, Konarskiego 18A, 44-100 Gliwice, Poland
[2] Łukasiewicz Research Network, Institute of Non-Ferrous Metals, Sowińskiego 5, 44-100 Gliwice, Poland
[3] Institute of Physics, University of Silesia, 75 Pułku Piechoty 1, 41-500 Chorzów, Poland
[4] Department of Physics, Czestochowa University of Technology, Armii Krajowej 19, 42-200 Częstochowa, Poland

Abstract. Al–Y–Fe amorphous and nanocrystalline alloys are characterized by a unique collection of diverse properties that are influenced by various factors, including heat treatment. In this paper, the effect of heat treatment on the structural changes and selected properties of Al–Y–Fe metallic glasses in the as-spun state is investigated. The structure of the $Al_{88}Y_7Fe_5$ and $Al_{88}Y_6Fe_6$ alloys was examined by means of X-ray diffraction (XRD) and Mössbauer spectroscopy (MS). Corrosion resistance of the samples was characterized using polarization tests in a 3.5% NaCl solution at 25°C. The effect of sodium chloride on the surface was studied with scanning electron microscopy (SEM) and energy-dispersive spectroscopy (EDS). The magnetic properties of Al-based alloys were explored using a vibrating sample magnetometer (VSM). It was revealed that the tested alloys show better properties after annealing than in the as-spun state. The annealing of the $Al_{88}Y_7Fe_5$ and $Al_{88}Y_6Fe_6$ alloys in the temperature range of 200 to 300°C improved the magnetic properties and corrosion resistance of these materials. After 3600 s, better E_{OCP} values were recorded for the $Al_{88}Y_6Fe_6$ and $Al_{88}Y_7Fe_5$ alloys after annealing at 300°C and 200°C, respectively. On the basis of the polarization tests, it was concluded that the electrochemical properties are better for $Al_{88}Y_6Fe_6$ alloys after annealing at 300°C.

Key words: Al–Y–Fe metallic glasses; heat treatment; structural test; corrosion resistance; magnetic properties.

1. INTRODUCTION

Lightweight alloys that exhibit high mechanical properties and relatively good corrosion resistance are in demand on a large scale in the aircraft, automotive, white goods and architectural industries. These characteristics are to be found in amorphous aluminum matrix alloys, which have properties superior to those of typical crystalline Al alloys, and which are characterized by greater flexibility in the composition of the alloy, making these materials attractive for practical applications [1, 2].

The properties of metallic glasses, including those based on Al, are closely connected with their structure, which is amorphous and metastable. During thermal activation, an amorphous structure decomposes, affecting changes in mechanical, magnetic and electrochemical properties of metallic glasses [3–5].

Heat treatment of amorphous alloys may consist of annealing leading to relaxation of the amorphous structure and annealing resulting in full crystallization of metallic glasses, which in this case is disadvantageous due to the degradation of the properties of such materials, including, for example, loss of high corrosion resistance, as well as a significant increase in brittleness, preventing their practical use. A process that is significantly more advantageous for metallic glasses is annealing, as a result of which the amorphous structure relaxes, as this phenomenon usually leads to preservation and sometimes even improvement of the desired physical and mechanical properties of metallic alloys [6–8]. The reasons for the properties of improvement of amorphous alloys after heat treatment are being constantly discussed; therefore, more research is needed in this area [1, 4, 9].

Considering that physical and chemical properties are extremely important for practical applications of aluminum-based metallic glasses as engineering materials, the aim of the present work is to investigate the influence of annealing conditions on changes in the structure and selected properties of $Al_{88}Y_7Fe_5$ and $Al_{88}Y_6Fe_6$ alloys casted by means of melt spinning.

The current work is a supplement to the studies carried out for Al–Y–Fe alloys. In previous reports, only the changes occurring in the structure of these alloys under the influence of heat treatment were analyzed, but the corrosion resistance and changes in the magnetic behavior of Al–Y–Fe alloying systems were not investigated under the influence of thermal activation.

*e-mail: monika.spilka@polsl.pl

Manuscript submitted 2022-09-27, revised 2022-12-07, initially accepted for publication 2022-12-30, published in April 2023.

© 2023 The Author(s). This is an open access article under the CC BY license (http://creativecommons.org/licenses/by/4.0/)

2. MATERIALS AND METHODS

The samples for the tests were ribbons of metallic glasses $Al_{88}Y_7Fe_5$ and $Al_{88}Y_6Fe_6$. The base alloys were produced by induction melting of the elements Al, Fe, and Y with a purity of 99.9% in a ceramic crucible. The elements had the form of pieces. The final ingots with a diameter of 30 mm were obtained. The mixture of elements was melted under inert gas atmosphere (argon 5.0).

From the ingots produced, by melting at the speed of a 30 m/s copper wheel, ribbons with a thickness of approximately 30 μm were obtained, which were then subjected to heat treatment, consisting of annealing at 200, 250 and 300°C for 30 minutes and subsequent cooling in an argon atmosphere.

Aluminum-based alloys in the as-spun and annealed states were subjected to structural tests using the following methods: X-ray diffraction (XRD) and Mössbauer spectroscopy (MS). Phase analysis was performed on the Rigaku Mini Flex 600 powder diffractometer, equipped with a D/TEX strip detector, where the Cu tube is the X-ray source. The diffractograms were recorded using a step data collection method with a scan range of 2 theta of 10° to 90°.

Mössbauer measurements were performed at ambient temperature using a ^{57}Fe nucleus on an MS96 spectrometer equipped with a linear ^{57}Co:Rh source (25 mCi), multichannel analyzer, absorber, and detector. The device was calibrated using α-Fe foil (thickness 30 μm) under room temperature conditions. Analysis and evaluation of the obtained Mössbauer spectra were performed using the WMOSS program (Ion Prisecaru, WMOSS4 Mössbauer Spectral Analysis Software, 2009–2016).

In order to investigate the corrosion resistance of $Al_{88}Y_7Fe_5$ and $Al_{88}Y_6Fe_6$ ribbons, an electrochemical method of determining the corrosion rate was used. Corrosion tests were performed at room temperature with the use of Autolab 302 N potentiostat in a 3.5% sodium chloride solution. Resistance of the samples in the 3.5% NaCl environment was measured in a measuring cell containing three electrodes (reference electrode – saturated calomel electrode (SCE); counter electrode – platinum rod; working electrode – sample). The dependence of the open circuit potential (E_{OCP}) on time (3600 s) was measured. The corrosion rate was determined by extrapolating Tafel curves on the basis of the correlation of the potential with the logarithm of the current intensity. Using the NOVA software version 1.11, the corrosion potential (E_{corr}), corrosion current density (j_{corr}) and corrosion rate (v_{corr}) were all calculated. The scan rate was 1 $mV \cdot s^{-1}$.

The evaluation of the surface of the ribbons after corrosion tests was carried out using the Supra 35 scanning electron microscope (SEM) by Carl Zeiss, and the chemical composition of the surface layer was determined with the energy dispersive spectrometer (EDS) by EDAX.

The magnetic nature of the $Al_{88}Y_7Fe_5$ and $Al_{88}Y_6Fe_6$ alloys after annealing was carried out using the LakeShore 7307 vibrating sample magnetometer (VSM). The tests were carried out over the magnetic field of up to 10 kOe at room temperature, and included coercive force (H_c) and saturation magnetization (M_s), which were determined from hysteresis loops.

3. RESULTS AND DISCUSSION

The amorphous structure of the $Al_{88}Y_7Fe_5$ and $Al_{88}Y_6Fe_6$ alloys after annealing at 200, 250 and 300°C was verified by X-ray diffraction (Fig. 1). The XRD patterns of the ribbons presented broad diffraction lines and contained diffraction peaks corresponding to α-Al phase (after annealing at 300°C) of which significantly less is observed in the $Al_{88}Y_6Fe_6$ alloy.

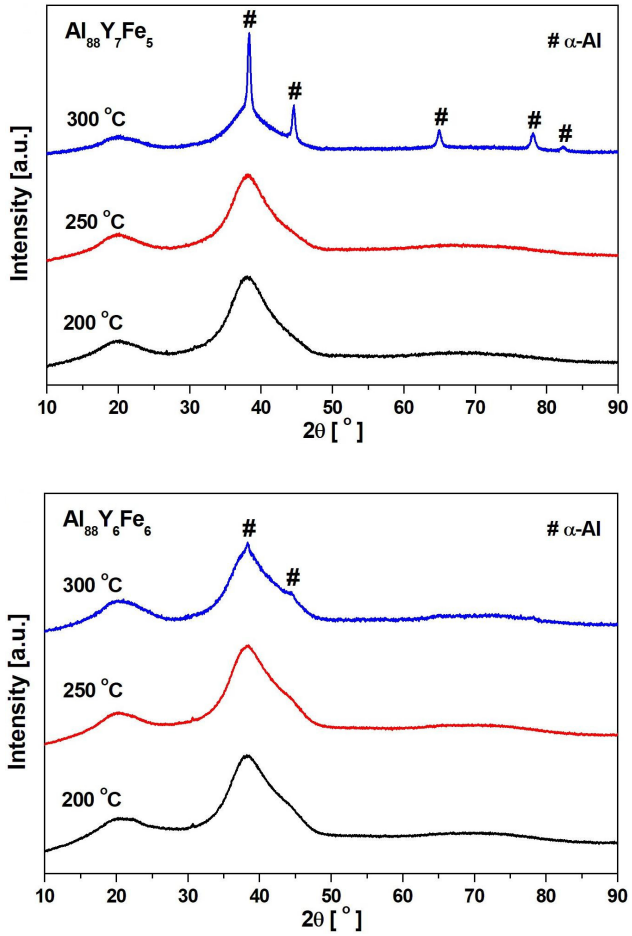

Fig. 1. X-ray diffraction patterns of $Al_{88}Y_7Fe_5$ (a) and $Al_{88}Y_6Fe_6$ (b) alloys after annealing at 200, 250 and 300°C

Similarly, the XRD analysis reported by Yang *et al.* [10] stated that nanosized aluminum crystals precipitate after isothermal annealing of the $Al_{88}Y_7Fe_5$ amorphous alloy at 280°C for 30 min, while increasing the annealing temperature to 370°C leads to further growth of aluminum crystals and precipitation of an $Al_{10}Fe_2Y$ intermetallic phase. Also, Saksl *et al.* [11] published the XRD pattern of the $Al_{88}Y_7Fe_5$ alloy after annealing at 773 K, which showed diffraction peaks corresponding to the fcc-Al, Al_3Y, and AlFeY phases. Based on other X-ray research carried out by Mudry *et al.* [12], it is established that at the first stage of primary crystallization (418–465 K) there is simultaneous nucleation and three-dimensional growth of Al nanocrystals. Therefore, by applying appropriate heat treatment, it is possible to obtain the microstructure of the amorphous alloy with nanograins of the base metal included in the amorphous matrix [13].

Room-temperature Mössbauer spectra for the studied samples in as-spun state and annealed at various temperatures are shown in Fig. 2. The spectra of all the alloys studied here are nearly symmetric and exhibit distribution of quadrupole splitting. These spectra were fitted well with two quadruple doublets, and the hyperfine parameters are listed in Table 1. The values of the isomer shift are almost the same for all components and are consistent with those expected for iron atoms in an Al rich environment [14–17]. Two components indicate that iron atoms are located correspondingly in two different neighborhoods of Al atoms. Based on XRD results and data from the literature [18], doublets with quadrupole splitting values of 0.42–0.49 mm/s reflect Fe atoms in Al-rich clusters. The second doublet, with much lower quadrupole splitting values, has hyperfine parameters characteristic of Fe present in Al–Y–Fe compounds [19, 20]. This doublet was interpreted as an amorphous phase. The annealing of the alloys at temperatures of 200°C and 250°C almost did not lead to a change in hyperfine parameters of the fitted components. However, after annealing at 300°C values of quadrupole splitting increase. This is probably due to the start process of the segregations accompanied by the onset of crystallization of amorphous parts of the samples.

To determine the influence of heat treatment on the corrosion resistance of the studied alloys, electrochemical tests using the potentiodynamic approach were provided. Figure 3 shows the results of measurements of the open-circuit potential (3a, c) and polarization curves (3b, d) for the cast alloys and after annealing.

The obtained values of open-circuit potential (E_{OCP}), corrosion potential (E_{corr}), corrosion current density (j_{corr}) and corrosion rate (v_{corr}) for $Al_{88}Y_7Fe_5$ and $Al_{88}Y_6Fe_6$ alloys were listed in Table 2.

Table 1

Hyperfine parameters of $Al_{88}Y_7Fe_5$ and $Al_{88}Y_6Fe_6$ alloys in as-spun state and after annealing at various temperatures (IS = isomer shift, QS = quadrupole splitting, A = relative area derived from the spectra). Absolute errors are estimated at ±0.01 mm/s for IS and ±0.02 mm/s for QS

Sample		IS (mm/s)	QS (mm/s)	A (%)	Component
$Al_{88}Y_7Fe_5$	as-spun	0.18	0.42	56	Doublet 1
		0.17	0.19	44	Doublet 2
	200°C	0.18	0.44	51	Doublet 1
		0.17	0.20	49	Doublet 2
	250°C	0.18	0.43	51	Doublet 1
		0.17	0.20	49	Doublet 2
	300°C	0.19	0.49	51	Doublet 1
		0.18	0.24	49	Doublet 2
$Al_{88}Y_6Fe_6$	as-spun	0.18	0.43	52	Doublet 1
		0.17	0.21	48	Doublet 2
	200°C	0.18	0.44	50	Doublet 1
		0.17	0.21	50	Doublet 2
	250°C	0.18	0.45	52	Doublet 1
		0.17	0.20	48	Doublet 2
	300°C	0.18	0.48	52	Doublet 1
		0.18	0.23	48	Doublet 2

The open-circuit and corrosion potential indicate when the corrosion processes in the investigated material started. With

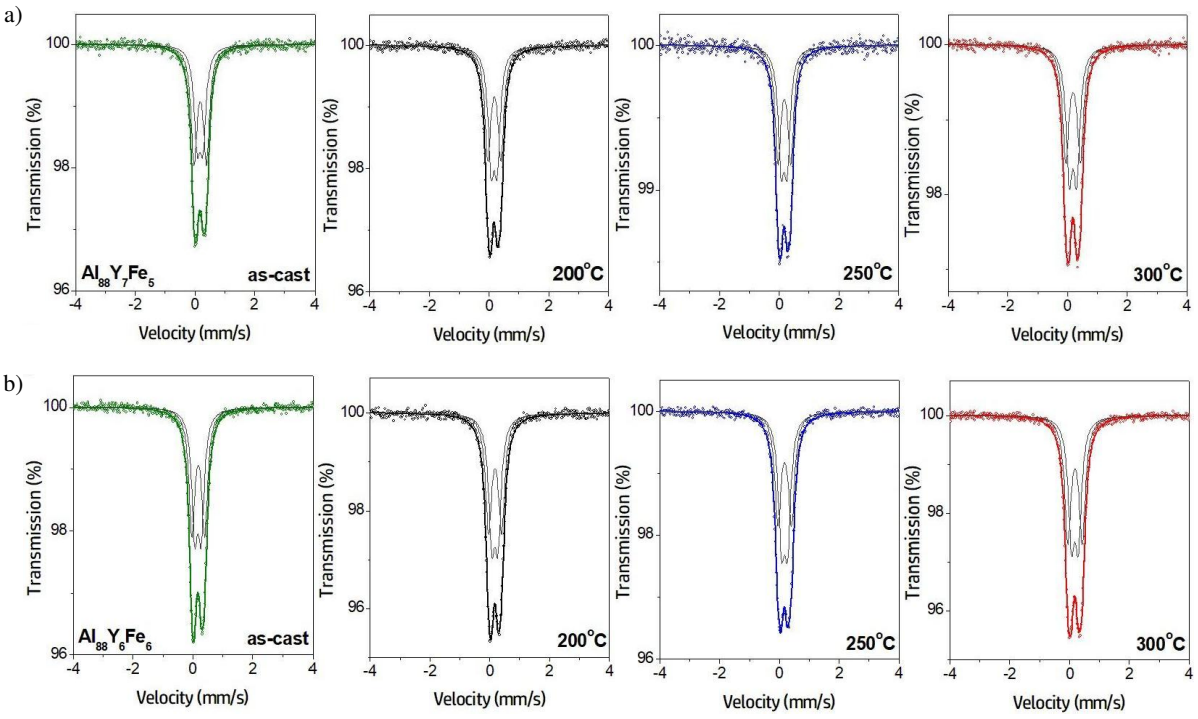

Fig. 2. Mössbauer spectra of $Al_{88}Y_7Fe_5$ (a) and $Al_{88}Y_6Fe_6$ (b) alloys in as-spun state and after annealing at 200, 250 and 300°C

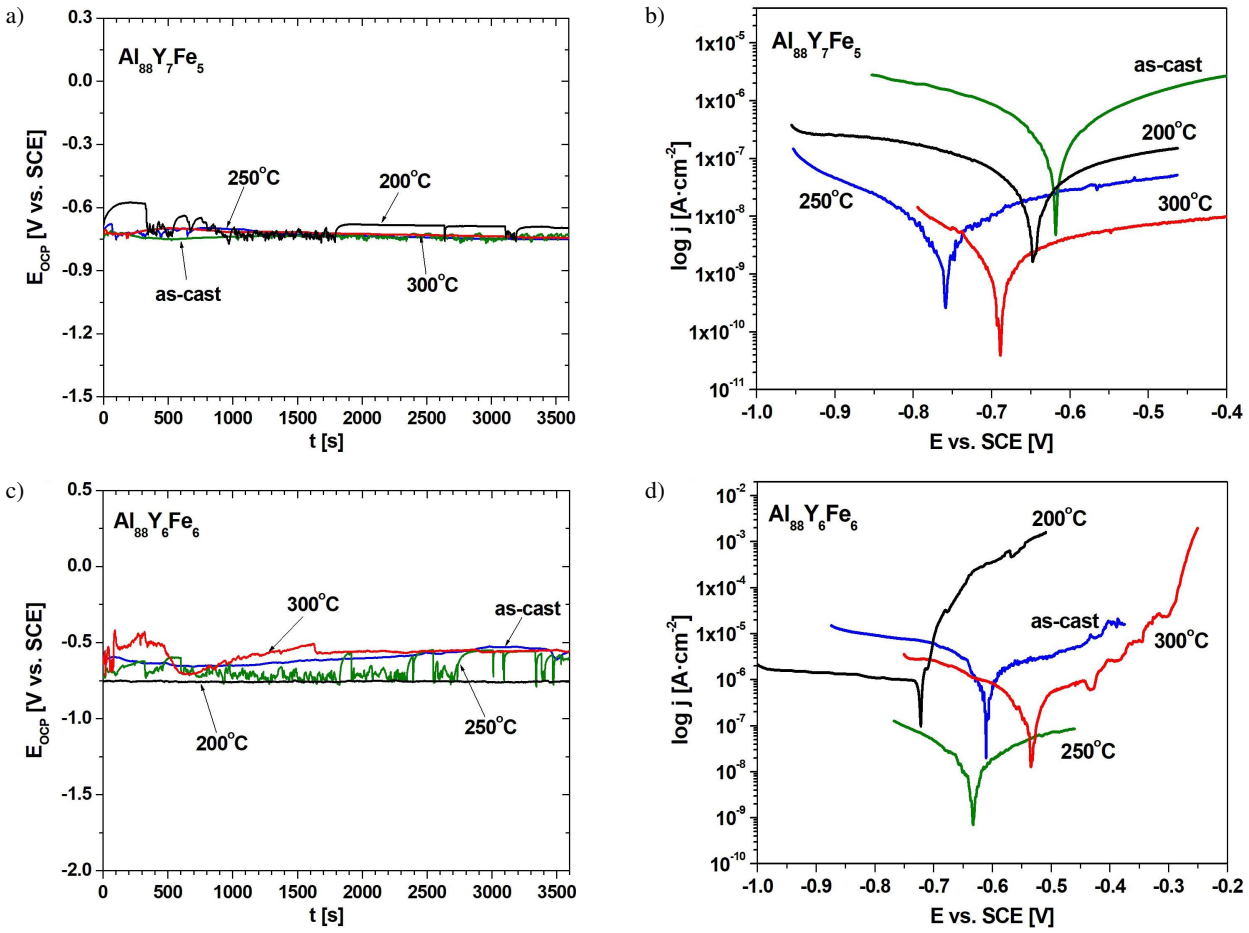

Fig. 3. Variations of open-circuit potential in a function of time (a, c) and polarization curves (b, d) in 3.5% NaCl solution at 25°C of $Al_{88}Y_7Fe_5$ alloy (a, b) and $Al_{88}Y_6Fe_6$ alloy (c, d)

Table 2

Electrochemical parameters of the $Al_{88}Y_7Fe_5$ and $Al_{88}Y_6Fe_6$ alloys in 3.5% NaCl solution at 25° in as-spun state and after annealing

Sample	Type	E_{OCP} [V] (±0.01)	E_{corr} [V] (±0.01)	j_{corr} [μA/cm^2] (±0.1)	v_{corr} [mm/year] (±0.001)
$Al_{88}Y_7Fe_5$	as-spun	–0.727	–0.618	0.31	0.011
	200°	–0.707	–0.645	0.03	0.001
	250°	–0.749	–0.763	0.01	0.0003
	300°	–0.745	–0.691	0.01	0.0005
$Al_{88}Y_6Fe_6$	as-spun	–0.561	–0.606	0.60	0.021
	200°	–0.756	–0.725	0.57	0.019
	250°	–0.599	–0.630	0.09	0.003
	300°	–0.555	–0.533	0.26	0.009

higher E_{OCP} and E_{corr} values, corrosion resistance of the tested material is greater. The changes in the open-circuit potential as a function of time showed an unstable nature in the studied materials. Better E_{OCP} values were recorded for the $Al_{88}Y_6Fe_6$ (−0.555 V) and $Al_{88}Y_7Fe_5$ alloys (−0.707 V) after annealing at 300°C and 200°C, respectively, than in the as-spun state.

Analysis of polarization curves of the as-spun and after-annealing samples indicates an increase in corrosion potential (E_{corr}) from −0.618 V for as-spun ribbon to −0.691 V for the sample annealed at 300°C and −0.763 V for the sample annealed at 250°C in the case of $Al_{88}Y_7Fe_5$ alloy.

For the $Al_{88}Y_6Fe_6$ alloy, the best value of the corrosion potential was noted for the sample annealed at 300°C (−0.533 V), while the lowest E_{corr} value was noticed for the ribbon annealed at 200°C (−0.725 V).

The corrosion current density exhibited the highest value for the $Al_{88}Y_6Fe_6$ alloy in the as-spun state ($j_{corr} = 0.60$ μA/cm^2) and after annealing at 200°C ($j_{corr} = 0.57$ μA/cm^2). In addition, the $Al_{88}Y_7Fe_5$ ribbon demonstrated a better value of corrosion current density ($j_{corr} = 0.31$ μA/cm^2) than the samples after annealing. The lowest j_{corr} values were obtained for the $Al_{88}Y_7Fe_5$ ribbon after annealing at 250 and 300°C. The corrosion current density is directly correlated with the corrosion rate. The lowest corrosion rate ($v_{corr} = 0.0003$ mm/year) was calculated for the $Al_{88}Y_7Fe_5$ alloy after annealing at 250°C, and the greatest weight loss was found for the $Al_{88}Y_6Fe_6$ alloy as-spun state ($v_{corr} = 0.021$ mm/year). The variable effect of the annealing process on the change in the corrosion resistance of Al-based amorphous alloys is confirmed by research carried out in [1, 3, 6, 21, 22]. [6] showed that after annealing at 523 K

of the amorphous $Al_{86}Ni_{10}Zr_4$ melt spun alloy, corrosion resistance of the ribbons improved. In turn, polarization tests of the $Al_{84}Ni_9Y_7$ alloy revealed the negative effect of heat treatment at 373 to 673 K on the corrosion resistance of these materials, because the samples tested after annealing exhibited a lower potential than the sample in the spun state [22]. Thus, corrosion resistance of the alloy is mainly dependent on its chemical composition and microstructure. The data in the literature indicate that glassy materials are characterized by better corrosion resistance, because the amorphous structure decreases structural heterogeneities as reasons for corrosion [1, 23]. This is confirmed by the research carried out. For the amorphous $Al_{88}Y_7Fe_5$ sample, better corrosion potential was declared as compared to the annealed samples. In turn, the electrochemical properties are better for the $Al_{88}Y_6Fe_6$ alloy after annealing at 300°C. Therefore, it could be concluded that high corrosion resistance can also be obtained after structural relaxation annealing or partial crystallization annealing [6]. Tailleart *et al.* [21] observed the best corrosion resistance of an amorphous Al-Co-Ce alloy after relaxation. In turn, Boichyshyn *et al.* [24] showed an increase in the corrosion resistance of Al-based amorphous alloys after the first stage of crystallization, when nanocrystals precipitated in the amorphous matrix. In $Al_{88}Y_7Fe_5$ and $Al_{88}Y_6Fe_6$ alloys after annealing at 300°C, the diffraction peaks corresponding to the α-Al phase precipitated in the amorphous matrix were identified. Thus, apart from the chemical composition, structure is the factor responsible for the behavior in an electrochemical environment.

The surface morphology of the ribbons after annealing at 300°C and after corrosion tests is shown in Fig. 4.

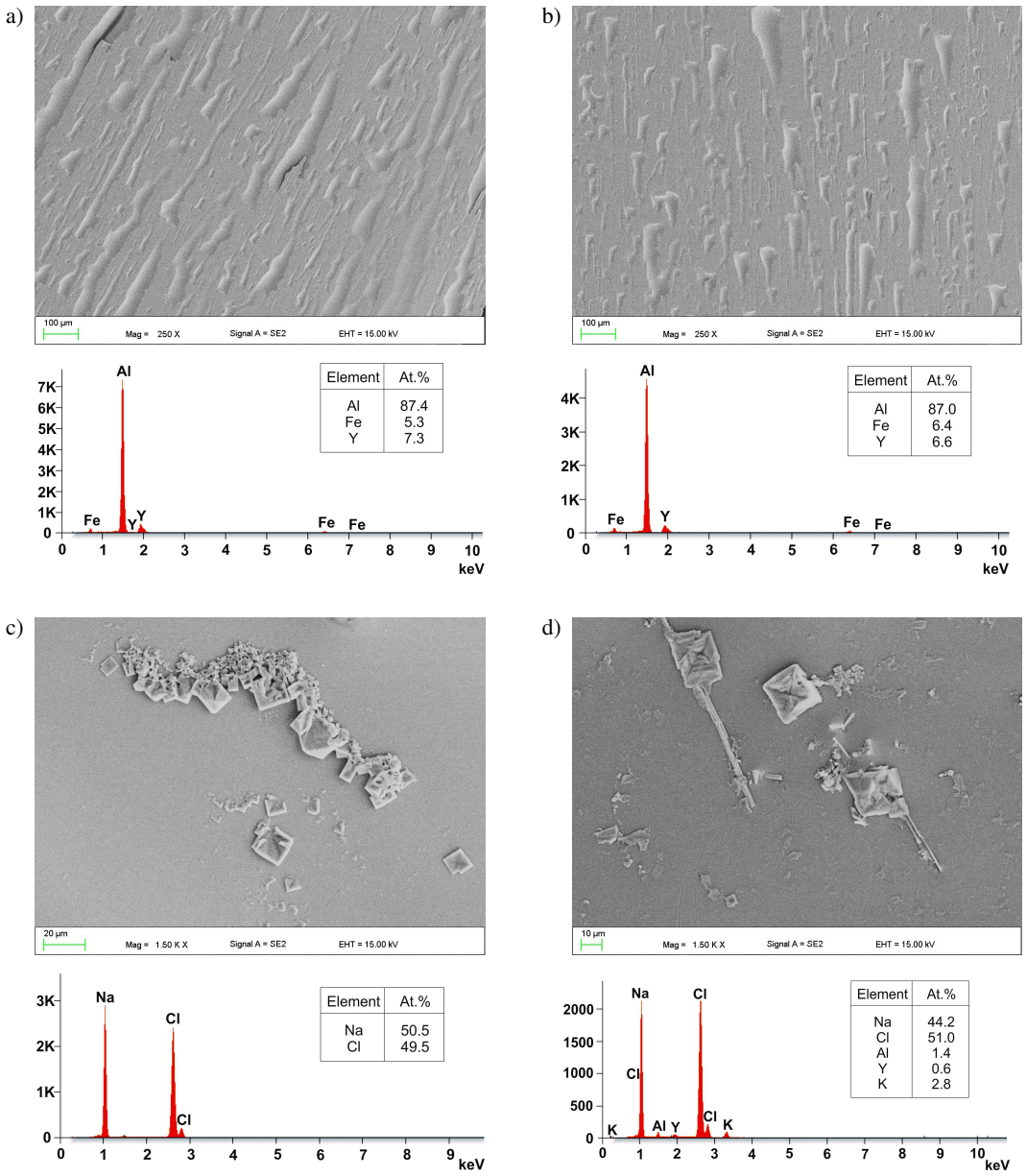

Fig. 4. SEM images and EDS spectra of the surface of $Al_{88}Y_7Fe_5$ (a, c) and $Al_{88}Y_6Fe_6$ (b, d) alloys after annealing at 300° (a, b) and after corrosion tests (c, d)

A large number of irregular gas pockets can be observed in the cast samples on the wheel side, which are evenly distributed on the surface of the ribbons (Fig. 4a, b). SEM observations showed that the surfaces of samples after corrosion tests are quite smooth and shiny, covered by NaCl crystals (Fig. 4c, d). No pits were observed. EDS analysis revealed the presence of sodium and chlorine, but did not confirm the presence of oxygen. The corrosion behavior of the $Al_{88}Fe_5Y_7$ alloy in 3.5% NaCl at room temperature was also studied by Yin *et al.* [25] using SEM and EDS analysis, and they reported the formation of an oxide film on the surface of the samples. In turn, Zhang *et al.* [6] investigated the corrosion morphology of the ribbons before and after heat treatment, immersing them in 3.5 wt% NaCl solution for 60 h and confirming the occurrence of only slight signs of local corrosion for the 523 K heat treatment sample. Similarly, Babilas *et al.* [22] observed that the surface of annealed $Al_{84}Ni_9Y_7$ ribbons after corrosion tests was free of pitting.

The magnetization behavior of the investigated Al-based alloys was evaluated using a VSM apparatus (Fig. 5).

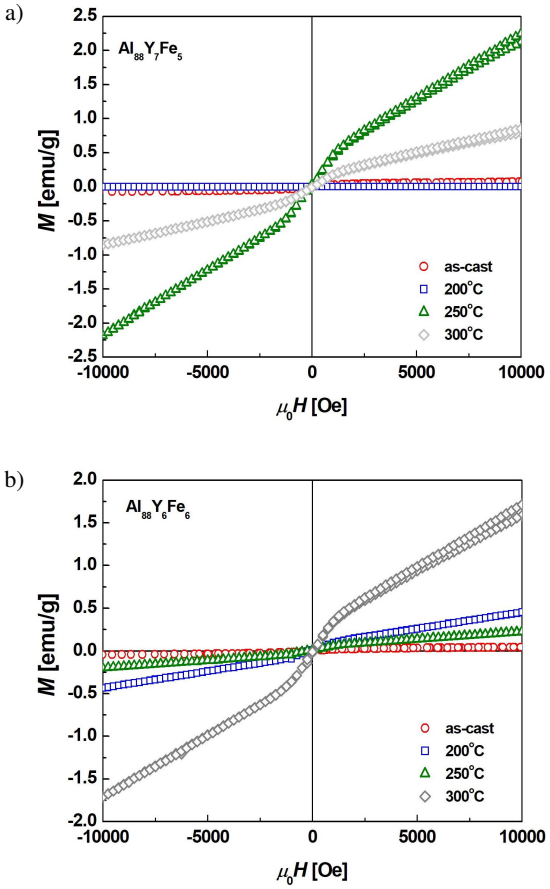

Fig. 5. Magnetic hysteresis loops of $Al_{88}Y_7Fe_5$ (a) and $Al_{88}Y_6Fe_6$ (b) alloys in as-spun state and after annealing at 200, 250 and 300°

Furthermore, the saturated magnetizations (M_s) and coercivity (Hc) values were listed in Table 3.

The $Al_{88}Y_7Fe_5$ alloy shows the best magnetic parameters after annealing at 250°C. In this state, ribbons exhibit the highest M_s value of 2.25 emu/g. The impact of heat treatment on the improvement of magnetic properties is noticeable. The exception is the sample of the $Al_{88}Y_7Fe_5$ alloy after annealing at 200°C, whose saturation magnetization value is the lowest (0.02 emu/g). It is different in the case of coercivity. Alloys in the as-cast state are characterized by a significantly higher value of H_c than after annealing. The highest value of H_c is exhibited by the $Al_{88}Y_6Fe_6$ as-spun alloy (127 Oe).

Table 3
Magnetic parameters of the $Al_{88}Y_6Fe_6$ and $Al_{88}Y_7Fe_5$ alloys in as-spun state and after annealing

Sample	Type	M_S [emu/g]	H_c [Oe]
$Al_{88}Y_7Fe_5$	as-spun	0.18	91
	200°	0.02	55
	250°	2.25	35
	300°	0.85	16
$Al_{88}Y_6Fe_6$	as-spun	0.14	127
	200°	0.45	15
	250°	0.22	41
	300°	1.59	12

Al-based amorphous alloys are not magnetic alloys [26], therefore, the magnetic properties of aluminum-transition metal-rare earth (Al–TM–RE) type metallic glasses have not been extensively studied. However, some of the Al-based amorphous alloys exhibit diamagnetism, frustration, spin glass behavior and superparamagnetism [27]. Chrobak *et al.* [28] analyzed the magnetic properties of the amorphous alloy $Al_{87}Y_5Ni_8$ under isothermal conditions at 300 and 2 K. Magnetization measurements of the alloy as a function of magnetic field (H; 0–7 T) showed that the curve, M(H), measured at 2 K saturates at a magnetic field value of about 1 T, but the isotherms recorded at 300 K do not exhibit saturation behavior at all. Therefore, it was concluded that the magnetic properties of the glassy alloy correspond to a superparamagnetic state with magnetic Ni clusters. In another study [29], the magnetic properties of amorphous alloys were investigated, and it was found that at room temperature the samples exhibit diamagnetic behavior, which is highly dependent on microstructure.

4. CONCLUSIONS

In the article, the structural as well as anticorrosion and magnetic properties of $Al_{88}Y_7Fe_5$ and $Al_{88}Y_6Fe_6$ alloys were investigated under different annealing conditions. Study of the structure of the annealed ribbons showed that the α-Al phase precipitated in the amorphous matrix at 300°C. A differential effect of heat treatment on selected properties of alloys obtained by means of melt spinning was also found. Both alloys in the melt-spun state exhibit the highest corrosion current density. The cast ribbon of $Al_{88}Y_7Fe_5$ alloy also obtained the most expected value of the corrosion potential. In the case of the $Al_{88}Y_6Fe_6$ alloy, annealing at 300°C improved the value of the corrosion

potential. Thus, the difference in corrosion resistance between as-spun and after annealing state of the studied alloys is mainly due to the microstructure, which was partially crystallized after heat treatment at 300°C. SEM images revealed no signs of pitting on the surface of the tested samples after annealing at 200 to 300°C, which allows for the use of these materials in the NaCl environment.

ACKNOWLEDGEMENTS

The work was supported by National Science Centre, Poland, under research project No.: 2018/29/B/ST8/02264.

REFERENCES

[1] L.M. Zhang *et al.*, "Thermally induced structure evolution on the corrosion behavior of Al-Ni-Y amorphous alloys," *Corrosion Sci.*, vol. 144, pp. 172–183, 2018, doi: 10.1016/j.corsci.2018.08.046.

[2] S.Y. Kim *et al.*, "High strength nanostructured Al-based alloys through optimized processing of rapidly quenched amorphous precursors," *Sci. Rep.*, vol. 8, p. 1090, 2018, doi: 10.1038/s41598-018-19337-7.

[3] R. Jindal, V.S. Raja, M.A. Gibson, M.J. Styles, T.J. Bastow, and C.R. Hutchinson, "Effect of annealing below the crystallization temperature on the corrosion behavior of Al–Ni–Y metallic glasses," *Corrosion Sci.*, vol. 84, pp. 54–65, 2014, doi: 10.1016/j.corsci.2014.03.015.

[4] J.H. Perepezko, M. Gao, and J.Q. Wang, "Nanoglass and nanocrystallization reactions in metallic glasses," *Front. Mater.*, vol. 8, 663862, 2021, doi: 10.3389/fmats.2021.663862.

[5] C. Fan, X. Yue, A. Inoue, C.T. Liu, X. Shen, and P.K Liaw, "Recent topics on the structure and crystallization of Al-based glassy alloys," *Mat. Res.*, vol. 22, no. 1, p. e20180619, 2019, doi: 10.1590/1980-5373-MR-2018-0619.

[6] S. Zhang *et al.*, "Crystallization behavior and corrosion resistance of $Al_{86}Ni_{10}Zr_4$ amorphous alloy under different annealing treatment conditions," *J. Non-Cryst. Solids*, vol. 593, pp. 121775, 2022, doi: 10.1016/j.jnoncrysol.2022.121775.

[7] A.G. Igrevskaya, A.I. Bazlov, N.Yu. Tabachkova, D.V. Louzguine, and V.S. Zolotorevskiy, "Influence of annealing at various temperatures on the structure and hardness of amorphous ribbons of the $Al_{85}Y_8Ni_5Co_2$ alloy," *Russ. J. Non-Ferrous. Met.*, vol. 59, no. 5, pp. 520–526, 2018, doi: 10.3103/S1067821218050061.

[8] K. Khrushchyk, L. Boichyshyn, and V. Kordan, "Influence of annealing on mechanical properties of alloys of Al-REM-Ni (Fe)," *Mater. Today: Proc.*, vol. 62, pp. 5739–5744, 2022, doi: 10.1016/j.matpr.2022.02.343.

[9] A. Aronin, D. Matveev, E. Pershina, V. Tkatch, and G. Abrosimova, "The effect of changes in Al-based amorphous phase structure on structure forming upon crystallization," *J. Alloy. Compd.*, vol. 715, pp. 176–183, 2017, doi: 10.1016/j.jallcom.2017.04.305.

[10] H. Yang, L. Luo, Y. Shen, and C. Li, "Glass forming ability and thermal stability of Al–Y–Fe amorphous alloys," *J. Shenyang. Univ. Technol.*, vol. 36, no. 5, pp. 498–502, 2014, doi: 10.7688/j.issn.1000-1646.2014.05.04.

[11] K. Saksl, P. Jóvári, H. Franz, "Atomic structure of $Al_{88}Y_7Fe_5$ metallic glass," *J. Appl. Phys.*, vol. 97, 113507, 2005, doi: 10.1063/1.1914955.

[12] S.I. Mudry, O. Kulyk Yu, and L.M. Boichyshyn, "Nanocrystallization of amorphous alloy $Al_{87}Ni_8Dy_5$ induced by heat treatment," *Mater. Today: Proc.*, vol. 62, pp. 5800–5804, 2022, doi: 10.1016/j.matpr.2022.03.493.

[13] L.M. Boichyshyn, Kh.I. Khrushchyk, M.O. Kovbuz, O.M. Hertsyk, and T.H. Hula, "Specific features of the transition of amorphous $Al_{87}REM_5Ni_8$(Fe) alloys into the crystalline state under the influence of temperature," *Mater. Sci.,* vol. 55, no. 1, pp. 17–26, 2019, doi: 10.1007/s11003-019-00246-7.

[14] R. Dunlap, K. Dini, G. Stroink, G. Collins, and S. Jha, "An Fe Mössbauer effect study of metastable $Al_{86}Fe_{14}$ prepared by rapid solidification," *Hyperfine Interact.*, vol. 28, pp. 963–966, 1986, doi: 10.1007/BF02061604.

[15] R. Dunlap, M. Yewondwossen, and D. Lawther, "Mössbauer effect studies of amorphous A1-Y-Ni-Fe alloys," *J. Non-Cryst. Solids*, vol. 156–158, pp. 192–195, 1993, doi: 10.1016/0022-3093(93)90161-P.

[16] E. Fazakas, S. Kane, K. Lazar, L. Varga, "Mössbauer study of rapidly solidified Al-Fe based amorphous alloys," *Hyperfine Interact.*, vol. 189, pp. 119–123, 2009, doi: 10.1007/s10751-009-9936-5.

[17] S. Kaloshkin *et al.*, "Composed phases and microhardness of aluminium-rich aluminium-iron alloys obtained by rapid quenching, mechanical alloying and high pressure torsion deformation," *Mater. Trans.*, vol. 43, pp. 2031–2038, 2002, doi: 10.2320/matertrans.43.2031.

[18] E. Kuzmann, A. Vertes, A. Griger, and V. Stefiiniay, "Mossbauer and X-ray study of rapidly quenched and mechanically alloyed AlFe alloys," *Hyperfine Interact.*, vol. 92, pp. 943–947, 1994, doi: 10.1007/BF02065716.

[19] G. Kalvius, F. Wagner, I. Halevy, and J. Gal, "The magnetism of rare earth intermetallics RFe_4Al_8," *Hyperfine Interact.*, vol. 151/152, pp. 195–207, 2003, doi: 10.1023/B:HYPE.0000020411. 32596.a6.

[20] J. Waerenborgh *et al.*, "Y–Fe–Al ternary system: partial isothermal section at 1070 K. Powder X-ray diffraction and Mossbauer spectroscopy study," *J. Alloy. Compd.*, vol. 323–324, pp. 78–82, 2001, doi: 10.1016/S0925-8388(01)00990-2.

[21] N.R. Tailleart, R. Huang, T. Aburada, D.J. Horton, and J.R. Scully, "Effect of thermally induced relaxation on passivity and corrosion of an amorphous Al-Co-Ce alloy," *Corrosion Sci.*, vol. 59, pp. 238–248, 2012, doi: 10.1016/j.corsci.2012.03.012.

[22] R. Babilas, A. Bajorek, M. Spilka, W. Łoński, and D. Szyba, "Electrochemical characterization of $Al_{84}Ni_9Y_7$ metallic glass after annealing process," *J. Non-Cryst. Solids*, vol. 518, pp. 24–35, 2019, doi: 10.1016/j.jnoncrysol.2019.04.042.

[23] R. Babilas, K. Młynarek-Żak, W. Łoński, D. Łukowiec, T. Warski, and A. Radoń, "Study of crystallization mechanism of Al.-based amorphous alloys by in-situ high temperature X-ray diffraction method," *Sci. Rep.*, vol. 12, 5733, 2022, doi: 10.1038/s41598-022-09640-9.

[24] L.M. Boichyshyn, O.M. Hertsyk, M.O. Kovbuz, T.H. Pereverzewa, and B.Ya. Kotur, "Properties of amorphous alloys of Al-REM-Ni and Al-REM-Ni-Fe systems with nanocrystalline structure," *Mater. Sci.*, vol. 48, no. 4, pp. 555–559, 2013, doi: 10.1007/s11003-013-9537-y.

[25] P.J. Yin *et al.*, "Effect of Au addition on intermetallics precipitation tendency and repassivation of $Al_{88}Fe_5Y_7$ glassy alloy," *Int. J. Electrochem. Sci.*, vol. 12, pp. 1288–1305, 2017, doi: 10.20964/2017.02.15.

[26] Y. Zhang *et al.*, "Correlation between glasses forming ability and density of states for the micro-alloying Al-based metallic glasses," *J. Alloy. Compd.*, vol. 826, 154237, 2020, doi: 10.1016/j.jallcom.2020.154237.

[27] D.N. Binh, N.T.H. Oanh, N.H.Viet, "The effect of Ni and Ti additions on the glass forming ability and magnetic properties of Al-Fe-Y alloy prepared by mechanical alloying," *J. Non-Cryst. Solids*, vol. 583, pp. 121–478, 2022, doi: 10.1016/j.jnoncrysol.2022.121478.

[28] A. Chrobak, B. Kotur, T. Mika, and G. Haneczok, "Effect of Gd and Fe doping on magnetic properties of $Al_{87}Y_5Ni_8$ amorphous alloy," *J. Magn. Magn. Mater.*, vol. 321, no. 18, pp. 2767–2771, 2009, doi: 10.1016/j.jmmm.2009.04.005.

[29] G. Li, W. Wang, X. Bian, L. Wang, J. Zhang, R. Li, and T. Huang, "Influences of similar elements on glass forming ability and magnetic properties in Al-Ni-La amorphous alloy," *J. Mater. Sci. Technol.*, vol. 26, no. 2, pp. 146–150, 2010, doi: 10.1016/S1005-0302(10)60024-2.